Available online at www.sciencedirect.com
ScienceDirect
Optics Communications 281 (2008) 3726–3731
OPTICS COMMUNICATIONS
www.elsevier.com/locate/optcom

Photosensitive post tuning of chalcogenide $Te_{20}As_{30}Se_{50}$ narrow bandpass filters

Weidong Shen [a,*], Michel Cathelinaud [b], Michel Lequime [b], Virginie Nazabal [c], Xu Liu [a]

[a] State Key Laboratory of Modern Optical Instrumentation, Zhejiang University, Hangzhou, 310027 Zhejiang, China
[b] Institut FRESNEL, UMR CNRS 6133, Université Paul Cézanne – Ecole Centrale Marseille – Université de Provence Domaine, Universitaire de Saint-Jérôme, 13397 Marseille Cedex 20, France
[c] Sciences Chimiques de Rennes, UMR CNRS 6226, Université Rennes 1, 35042 Rennes, France

Received 26 November 2007; received in revised form 24 March 2008; accepted 25 March 2008

Abstract

We present an experimental study on the photosensitive properties of narrow bandpass filters based on a chalcogenide $Te_{20}As_{30}Se_{50}$ (TAS) spacer. The transmittance curve of single TAS layer was shifted towards long wavelength direction after 2 h exposure by Xenon arc lamp. The refractive index and extinction coefficient were both increased together with a red shift of optical gap. A maximum 1.7% photo-induced effect was observed. Narrow band filters constituted by TAS and cryolite were manufactured by electron beam deposition. The transmittance spectrum of the filter during the exposure by a wide band source was in situ measured and the resonant wavelength was observed to turn longer gradually till saturation. A spatially localized central wavelength change up to 5.7 nm was finally obtained. The stability of the photo-induced effect was studied and some comments were given at the end of this paper.

PACS: 42.79.Wc; 42.70.Gi

Keywords: Thin film filter; Photosensitive material; Photo-induced change; Post tuning

1. Introduction

Narrow bandpass filters (NBFs) are one of the key components in optics communications, fluorescence excitation/detection and laser-line cleaning. Today, as high energy deposition technologies like ion assisted deposition (IAD) or dual ion beam sputtering (DIBS) develop, most of the well-designed NBFs can be manufactured by optical monitoring with error compensation [1]. However, due to the high requirements on error tolerance and the limit of thickness uniformity in the deposition chamber, the production yield is still very low. Generally, there is only one circular ring on the whole substrate which will satisfy the final performance. Thus, the use of a photosensitive material for the spacer of NBFs [2] would be very attractive for enabling the post trimming of such devices with the help of a light beam. It could not only correct the consequences of some deposition errors on the filter properties accurately, but also create entirely new filtering devices with controlled spatial properties, for instance, variable filters with arbitrary profile or apodizing filter with spatially-structured transmission/reflectance response.

The chalcogenide glasses are transparent in the near- and mid-infrared regions of the spectrum (0.5−10 μm for sulphides, 0.8−12 μm for selenides, up to 20 μm for tellurides) and present high refractive index typically in the range of 2.0–2.9 at 1.5 μm [3]. Therefore it can be used as high index material for the manufacturing of narrow bandpass filters in the near infrared region [4]. Moreover, the photosensitivity of chalcogenide materials has been successfully utilized for the creation of directly written waveguides [5–8], strong

* Corresponding author. Tel.: +86 571 87951190.
E-mail address: adongszju@hotmail.com (W. Shen).

0030-4018/$ - see front matter © 2008 Elsevier B.V. All rights reserved.
doi:10.1016/j.optcom.2008.03.041

Bragg gratings [9,10] and post-tuning of photonic crystal waveguides [11,12]. We have previously reported light trimming of NBFs based on photosensitive $Ge_{15}Sb_{20}S_{65}$ spacer in which a 5.4 nm blue shift of central wavelength could be observed with light exposure around 480 nm and an ultra-uniform filter was finally obtained by post trimming [13]. In this paper, the photosensitivity of $Te_{20}As_{30}Se_{50}$ (TAS) narrow band filter was studied. TAS has a low optical gap ($E_{gap} = 1.46$ eV), a low glass transition temperature ($T_g =$ 137 °C) and a high refractive index ($n = 3.0$ @1550 nm). Opposite to $Ge_{15}Sb_{20}S_{65}$, photo-induced change of a red shift was obtained for single TAS layer. In the vacuum deposition chamber, the optical properties of NBFs based on TAS spacer were in situ recorded during exposure. A 5.7 nm central wavelength shift towards longer direction was observed. At the end, the localization and stability of the photo-induced change was investigated.

2. Study of single TAS layer photosensitivity

The photosensitivity of the chalcogenide is known to arise from structural rearrangements induced by the single photon absorption of light at frequencies near or below the optical gap of the material [14]. These structural rearrangements lead to the changes of the refractive index. The magnitude and sign of the photo-induced changes are highly dependant on the chemical composition of chalcogenide material. To identify the specific photosensitivity of TAS, a single layer of this material was first studied. Typical equipment of electron beam deposition (EBD) used for the preparation of coatings was a Balzers BAK 600 evaporation plant with a 60-cm stainless steel bell jar and two electron beam guns with water-cooled crucibles. TAS materials were placed in a graphite crucible of 4-cc capacity. An x–y sweep could be used to increase the film uniformity. The film was deposited on fused silica substrate that was subjected to a normal cleaning procedure prior to being cleaned by a discharge in vacuum chamber. The distance from the source to substrates was around 50 cm. Controlled by a quartz sensor, deposition took place at a rate of 1 nm/s with a pressure of 2×10^{-6} mbar. The total thickness of single layer was about 630 nm monitored by optical transmittance method.

After deposition, the single layer was exposed for 2 h by a Xenon arc lamp which provides a high intensity in a wavelength range between 400 nm and 1000 nm. The transmittance spectrums of this single layer before and after exposure were measured from 600 nm to 1700 nm with a 1 nm interval on a spectrophotometer previously developed in our team [15] which allows localized transmission and reflection measurements. As Fig. 1 shows, the transmission curve after light exposure was slightly shifted toward the long wavelength direction, which reveals a photo-induced increase of the optical thickness of the TAS film. It can be also seen that the transmittance values in short wavelength region were decreased a little after exposure (from 31.2% to 26% @800 nm). It indicates that the absorption was increased.

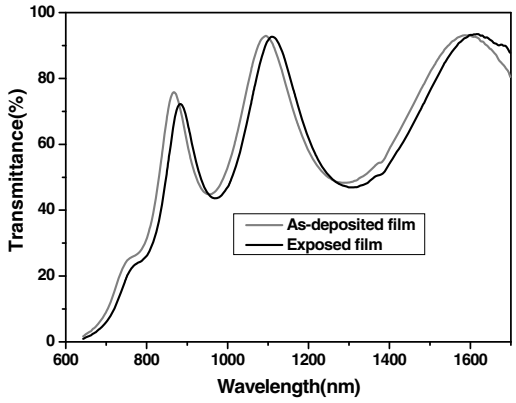

Fig. 1. The measured transmittance curves of as-deposited and exposed TAS single layers.

The optical constants, i.e., refractive index (n) and extinction coefficient (k), were determined by the spectral curve fitting method with a global optimization algorithm [16]. A Forouhi–Bloomer formula [17] was used to describe the dispersion of TAS material. The variation of mechanical thickness would only induce a shift of the whole transmission curve while the variations of optical constant could also influence the transmittance values especially at extreme points. As it could be seen from Fig. 1, the transmittance at a quarter-wavelength point near 1300 nm was decreased after illumination and it indicated refractive index was increased. So the photometric method could distinguish the variations of optical constant from mechanical thickness. The results of this determination are presented in Fig. 2. The refractive index and extinction coefficient in the whole spectral region were increased after exposure. The changes are respectively $\Delta n = 0.048$ at 1.55 μm and $\Delta k =$ 0.02 at 800 nm, with no obvious change of the film mechanical thickness (from 549 nm to 550 nm).

The optical gap of amorphous TAS could be determined from the absorption curve of the deposited film [18]. In high absorption region with $\alpha > 10^4$ cm^{-1} (absorption coefficient $\alpha = 4\pi k/\lambda$) involving optical transitions between conduction and valence band states, the absorption could be described by the following formula:

$$\alpha h\nu = B(h\nu - E_g^0)^m \quad (1)$$

where $h\nu$ is photon energy, E_g^0 is optical gap and B is a constant. The exponent m depends on the nature of the transition, and $m = 1/2$, 2, 3/2 or 3 for allowed direct, allowed non-direct, forbidden direct or forbidden non-direct transitions respectively. For TAS, it could be seen in Fig. 3 that there was a good linear relationship between $(\alpha h\nu)^{0.5}$ and $(h\nu)$ when $m = 2$, i.e., allowed non-direct transition. By extrapolating the linear portions to $(\alpha h\nu)^{1/2} = 0$ in the plots of $(\alpha h\nu)^{0.5}$ versus $(h\nu)$, the optical gap could be obtained. As Fig. 3 showed, E_g^0 was 1.56 eV (794.9 nm) and 1.54 eV (805.2 nm) respectively for as-deposited and exposed film. It meant that the optical gap was reduced (a red shift) after exposure.

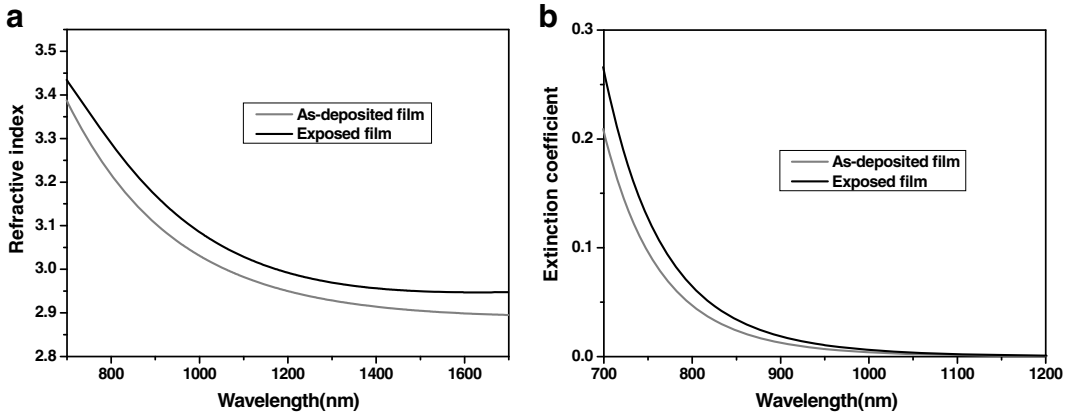

Fig. 2. The determined optical constants of as-deposited and exposed films. (a) Refractive index, (b) extinction coefficient.

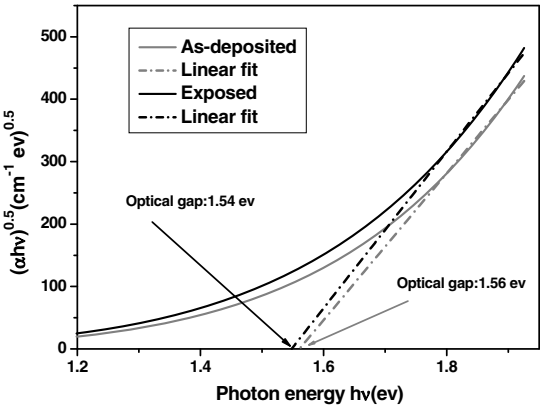

Fig. 3. $(\alpha h\nu)^{0.5}$ versus $(h\nu)$ of as-deposited and exposed TAS film.

All these photo-induced changes were perhaps caused by structural changes [14]. It is well known that practically all chalcogenides deposited by PVD methods go down in a highly non-equilibrium state which can be relaxed by thermal or photo annealing. Refractive index is commonly increased as they relax into a bonding structure closer to the equilibrium state. Additionally changes in the bandgap are commonly seen as this relaxation process proceeds (also giving changes in absorption). The formation of defects and localized electronic states in the tails of conduction and valence bands which lower the energy gap, i.e., photo-darkening effect, maybe also cause the change of optical constants [9]. The mechanism of the photo-induced change is still under investigation.

3. Post tuning of a narrow bandpass filter

For a dielectric Fabry-Perot filter, the resonant wavelength is mainly determined by optical thickness of the spacer layer. The relationship between central wavelength shift and spacer variation could be described by equation [19]:

$$\frac{\Delta\lambda}{\lambda_0} = \kappa\frac{\Delta(nd)}{(n_0 d_0)} \tag{2}$$

where λ_0 is central wavelength and $(n_0 d_0)$ is optical thickness of the spacer. κ is a positive coefficient, typically between 0.3 and 1, whose exact value is connected to the structure of high reflection mirror and there are analytical formulas for various filters [20]. This equation indicates that central wavelength shift $\Delta\lambda$ is linearly dependent on optical thickness change $\Delta(nd)$ of the spacer. If the spacer is photosensitive, we can modify locally index of the spacer layer and consequently the value of central wavelength of NBFs by a light beam with the required spot size and fluence.

Narrow bandpass filters $(PL)^3$ 6P $(LP)^3$ using TAS material as a photosensitive spacer were manufactured by electron beam evaporation where P and L were respectively a quarterwave of TAS and cryolite (Na_3AlF_6) at $\lambda_0 =$ 1550 nm. Na_3AlF_6 ($n = 1.3$) was chosen as a low index material because of its good compatibility with TAS. Fig. 4 shows the cross-section SEM images of the manufactured filter. It reveals the amorphous structure of TAS film deposited by EBD method. The chemical composition of this coating (Te:As:Se = 19.8:30.9:49.3) measured by an energy-dispersive X-ray analyzer was in good agreement with that of bulk glass (Te:As:Se = 20.5:29.5:50) [4]. A good interface between TAS and cryolite layers could be also observed. The optical monitoring with turning point method @1550 nm [21] was used to control the thickness of each layer. To avoid photo-induced change by light exposure near the optical gap (795 nm) of TAS material, a long-pass color filter (Schott RG830) was inserted in the light path of monitoring system during deposition as shown in Fig. 5.

After the manufacturing, the transmittance measurement from 1520 nm to 1570 nm was performed by in situ measurement system in vacuum chamber (Fig. 5). Fig. 6 shows the measured curve. The central wavelength, the bandwidth, and the maximum transmittance are 1550.6 nm, 4.9 nm and 91.2% respectively. There is a little difference between the measured and design data due to the thickness error and scattering loss.

The photosensitive response of this NBF was in situ measured in the vacuum chamber just after the manufacturing. As Fig. 5 shows, the light source is a halogen lamp

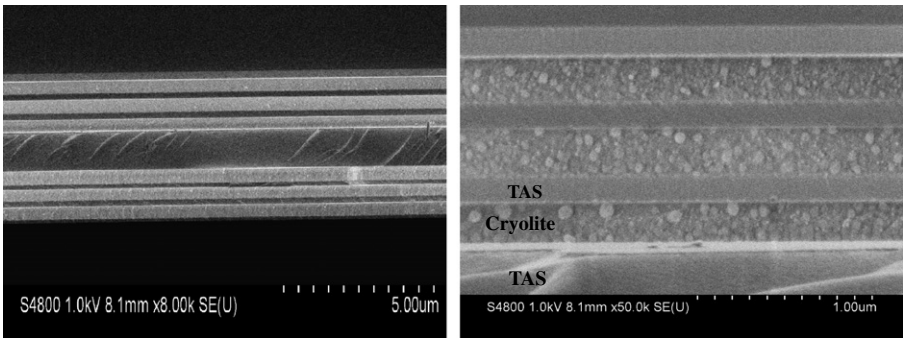

Fig. 4. Cross-section SEM images of the manufactured filter constituted by TAS and cryolite films.

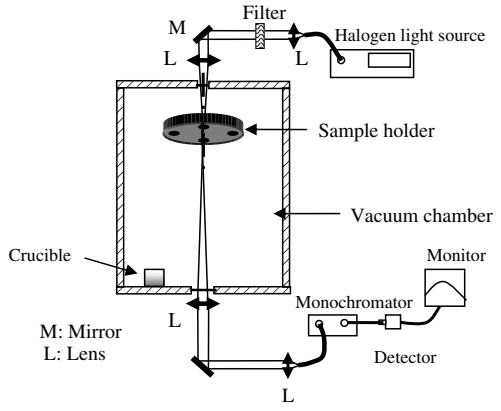

Fig. 5. Schematic graph of in situ transmittance measurement in vacuum chamber.

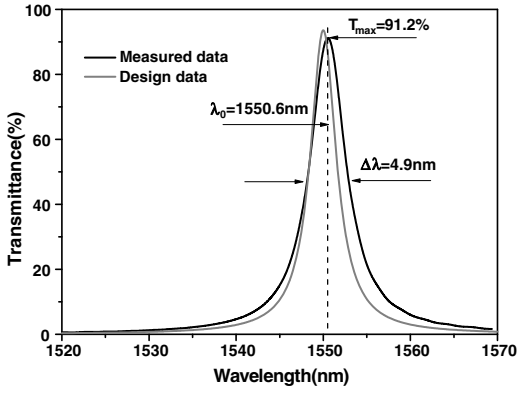

Fig. 6. The measured transmittance of TAS/Cryolite filter in the spectral range of 1520–1570 nm.

which provides a high intensity from 400 nm to 900 nm and the diameter of light beam is 4 mm. The exposure was performed by removing the RG830 filter. The transmittance during the exposure was measured every 2 h. Fig. 7a shows the recorded spectrum at different times. The transmittance curve was observed to shift gradually towards longer wavelength with increasing exposure. It indicated a positive photo-induced index change which was in accordance with the previously obtained results of single TAS layer. There was no obvious variation of the peak transmittance T_{max} during the exposure. Fig. 7b shows a plot of the central wavelength versus accumulated exposure time. The resonant wavelength shifted quickly at first but displays saturation behavior at longer time. This curve could be well fitted by an exponential equation as shown in Fig. 7b. The maximum wavelength shift finally reached 5.7 nm. The photosensitive response of NBF exposed by a laser-line of wavelength below or near the optical gap will be studied in the future and it is expected to reduce the exposure time greatly.

After the exposure, the filter was taken out from the chamber. A central wavelength mapping near the exposed area of NBFs was carried out on a dedicated mapping bench developed in our team which uses a C-band tunable laser and an InGaAs detector for transmittance measurement [22]. A small probing beam size of 400 μm was used for scanning with a 400 μm interval. Fig. 8 shows the central wavelength distribution recorded in an 8×8 mm^2 area (441 points). A local central wavelength peak of 4 mm diameter could be clearly observed and the central wavelength change almost perfectly reproduces the shape of the exposure light beam.

The stability of the photo-induced effect is important for the future application. To investigate the stability, the transmittance of TAS filter at the exposed area was measured automatically every 4 h on the same tunable laser bench where a temperature controller with 0.02 °C accuracy was used to hold the sample [16]. This measurement was performed in a black room in order to avoid possible background light influence. Fig. 9 shows the central wavelength variations for 7 days duration. The maximum change was 0.04 nm, with no drift evidence. This variation maybe results from a lack of repeatability in the positioning, moisture absorption effects or laser instability. However, it should be noted that this filter could be used only in a spectral region far away from the optical gap of photosensitive material (e.g. C-band for telecommunication) in order to avoid spontaneous change of optical properties induced by exposure [13]. It can be easily obtained by adding to the processed filter some colored glasses having a high absorbance in the specific spectrum.

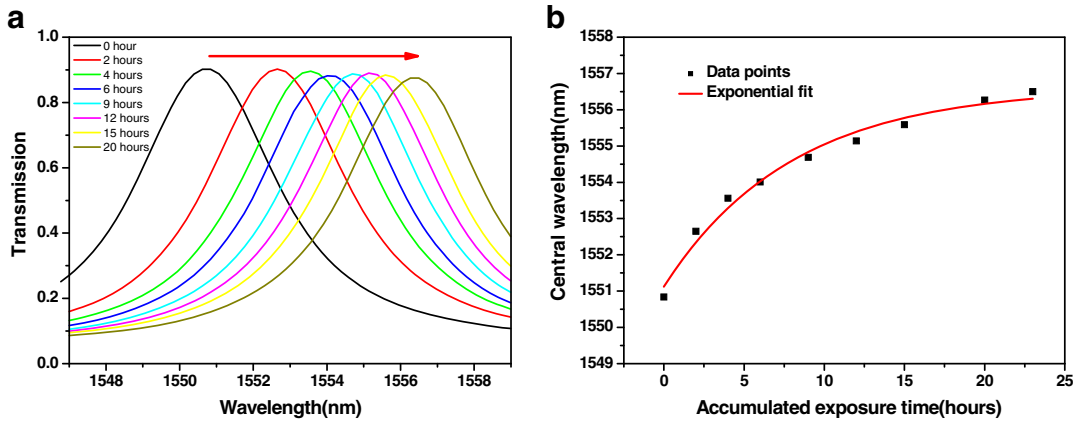

Fig. 7. (a) Measured NBF transmittance curves at different accumulated time of exposure. (b) Shift of the central wavelength versus accumulated exposure time.

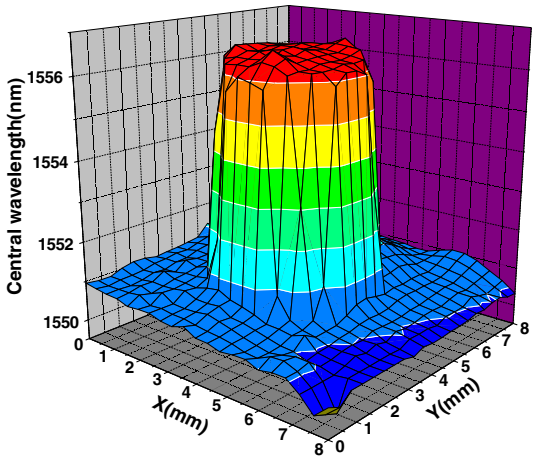

Fig. 8. Spatial variation of the NBF central wavelength after the exposure.

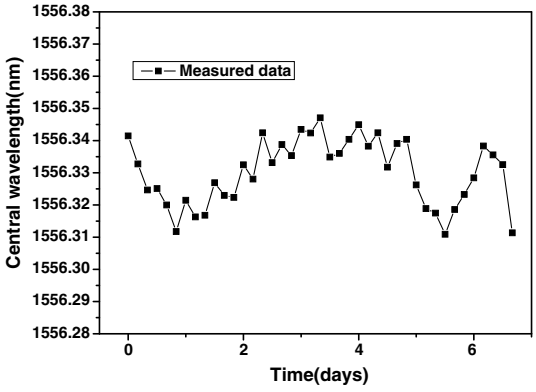

Fig. 9. NBF central wavelength variations at the trimmed area for 7 days duration.

4. Conclusion

In conclusion, we present an experimental demonstration of post tuning of NBFs based on photosensitive $Te_{20}As_{30}Se_{50}$ material. The photosensitivity of single TAS layer was first studied. After 2 h exposure by Xenon arc lamp, the transmittance curve was shifted towards long wavelength direction. The refractive index and extinction coefficient were both increased, together with a red shift of optical gap. A maximum 1.7% photo-induced change was observed. After that, narrow band filters constituted by TAS and cryolite were manufactured by electron beam deposition. The transmittance spectrum of the filter during the exposure by a wide band source was in situ measured and the resonant wavelength was observed to turn longer gradually till saturation. A spatially localized central wavelength change up to 5.7 nm was finally obtained. Multi-cavity narrow band filters with high cut-off properties should be usually designed for some applications, e.g., optics communication and laser-line cleaning. For this case, it will be very difficult to accurately control refractive index changes of each spacer layer during the light exposure. Different photosensitive material may be chosen as the cavity layers, and then the post-tuning could be performed at separate light illuminations according to each spacer's active wavelength. This post-processing technique is promising for thin film filter manufacturing either to correct the deposition error or create new spatially-structured filters.

Acknowledgements

It is a pleasure for authors to acknowledge the funding support from National Natural Science Foundation of China (No. 60708013). We also thank the Post-Doctoral funding of Centre National de la Recherche Scientifique (CNRS) in France.

References

[1] C.C. Lee, K. Wu, Opt. Lett. 32 (2007) 2118.
[2] M. Lequime, J. Lumeau, Proc. SPIE 5963 (2005) 60.

[3] S.R. Elliott (Ed.), Physics of Amorphous Materials, Longman, Essex, 1995.
[4] V. Nazabal, M. Cathelinaud, W.D. Shen, P. Nemec, F. Charpentier, H. Lhermite, M.L. Anne, J. Capoulade, F. Grasset, A. Moreac, S. Inoue, M. Fruman, J.L. Adam, M. Lequime, C. Amra, Appl. Opt. 47 (2008) C114.
[5] J.F. Viens, C. Meneghini, A. Villeneuve, T.V. Galstian, E.J. Knystautas, M.A. Duguay, K.A. Richardson, T. Cardinal, J. Lightwave Technol. 17 (1999) 1184.
[6] A.M. Ljungstrom, T.M. Monro, J. Lightwave Technol. 20 (2002) 78.
[7] D.A. Turnbull, J.S. Sanghera, V. Nguyen, I.D. Aggarwal, Mater. Lett. 58 (2004) 51.
[8] S. Ramachandran, S.G. Bishop, IEEE J. Sel. Top. Quantum Electron. 11 (2005) 260.
[9] A. Saliminia, A. Villeneuve, T.V. Galstyan, S. LaRochelle, K. Richardson, J. Lightwave Technol. 17 (1999) 837.
[10] M . Shokooh-Saremi, V. Taeed, I. Littler, D. Moss, B. Eggleton, Y. Ruan, B. Luther-Davies, Electron. Lett. 41 (2005) 13.
[11] T.K. Sudoh, Y. Nakano, K. Tada, IEEE J. Sel. Top. Quantum Electron. 3 (1997) 577.
[12] M.W. Lee, C. Grillet, C.L.C. Smith, D.J. Moss, B.J. Eggleton, D. Freeman, B. Luther-Davies, S. Madden, A. Rode, Y.L. Ruan, Y.H. Lee, Opt. Express 15 (2007) 1277.
[13] W.D. Shen, M. Cathelinaud, M. Lequime, F. Charpentier, V. Nazabal, Opt. Express 16 (2008) 373.
[14] A. Zakery, S.R. Elliott, J. Non-Cryst. Solids 330 (2003) 1.
[15] L. Abel-Tiberini, F. Lemarquis, M. Lequime, App. Opt. 45 (2006).
[16] F. Lemarchand, C. Deumie, M. Zerrad, L. Abel-Tiberini, B. Bertussi, G. George, B. Lazarides, M. Cathelinaud, M. Lequime, C. Amra, Appl. Opt. 45 (2006) 1312.
[17] A.R. Forouhi, I. Bloomer, Phys. Rev. B 38 (1988) 1865.
[18] A.A. Othman, Thin Solid Films 515 (2006) 1634.
[19] M. Lequime, R. Parmentier, F. Lemarchand, C. Amra, Appl. Opt. 41 (2002) 3277.
[20] W.D. Shen, X. Liu, B.Q. Huang, Y. Zhu, P.F. Gu, J. Opt. A-Pure Appl. Opt. 6 (2004) 853.
[21] H.A. Macleod, Thin-Film Optical Filters, third ed., Institute of Physics Publishing, Philadelphia, 2001.
[22] J. Lumeau, M. Lequime, Appl. Opt. 45 (2006) 6099.